Extended Abstracts of the 2017 International Conference on Solid State Devices and Materials, Sendai, 2017, pp1013-1014

PS-13-04

Impact of Crystallinity of AlN Thermal Conductive Film on Thermoelectric Power of Silicon Nanowire Micro Thermoelectric Generator

Ryo Yamato [1], Shuichiro Hashimoto [1] Tianzhuo Zhan [1] , Shunsuke Oba[1], Yuya Himeda[1], Takashi Matsukawa [2], and Takanobu Watanabe [1]

[1] Waseda Univ.
3-4-1, Ohkubo, Shinjuku-ku, Tokyo 169-8555, Japan
Phone: +81-3-5286-1621 E-mail: hazard-17@toki.waseda.jp
[2] AIST
1-1-1, Umezono, Tsukuba-shi, Ibaraki 305-8568, Japan

Abstract

We investigated the impact of the deposition processes of AlN thermal conductive (TC) film on the thermoelectric (TE) performance of Si nanowire micro thermoelectric generator (SiNW-μTEG). Two different processes are compared: 1) non-reactive RF sputtering using AlN target in Ar gas and 2) reactive RF sputtering using Al target in Ar/N_2 mixture gas. The TE power is found to be enhanced in the μTEGs with the synthesized AlN from Al target. The temperature drop across the SiNWs was larger in the μTEG with the reactively sputtered AlN than in the other one, suggesting that the reactively sputtered AlN has smaller thermal resistance. X-ray diffraction measurements revealed the reactively sputtered AlN has a higher crystallinity than that of the non-reactively sputtered AlN. These results show that the controlling crystallinity of TC film is effective to improve the TE power of the μTEGs.

1. Introduction

Researches on energy harvesting technology for extracting electric energy from environmental heat energies are promoted to realize IoT (Internet of Things) society based on trillion-sensor network. In recent years, it has been reported that silicon nanowire (SiNW) has suppressed thermal conductivity maintaining electrical conductivity [1-3]. This finding opens up SiNW-based micro thermoelectric generators (μTEGs) fabricated by CMOS-compatible process. In order to improve the TE power, it is important to reduce parasitic thermal resistance around the TE legs.

Aluminum nitride (AlN) is an electrical insulating material having a high thermal conductivity and a similar thermal expansion coefficient with that of Si [4,5]. This suggests AlN is suitable for a thermal conductive (TC) film of the μTEGs. However, the impact of the deposition process of TC films on the TE property had not been fully investigated. In this study, we fabricated two types of μTEGs having AlN TC films deposited by different processes, and compared the TE properties.

2. Experimental

Fig. 1 shows a schematic of our fabricated μTEGs. 400 SiNWs are fabricated on SOI substrate, both end of them are connected to electrode pads. Definition width and length of NWs are 100 nm and 8 μm, respectively. AlN TC film was deposited on one of the pads to conduct the heat current from the hot source. Fig. 2 shows the optical microscopy and SEM images of the μTEG.

The SiNWs were patterned on SOI wafer with a 45 nm thick SOI and a 145 nm thick buried oxide (BOX) by electron beam (EB) lithography and dry etching. Subsequently, dry thermal oxidation was performed at 850 °C for 3 hours. Thereafter, P ions were implanted at a dose of 1.0×10^{15} ions/cm^{-2}. The Si pad and the both ends of the SiNWs are nickelized. Finally, a 550－560 nm thick AlN film was deposited by RF sputtering. The one AlN film was deposited in Ar ambient using AlN target (nonreactively-sputtered AlN). The other was deposited in Ar/N_2 mixture gas using Al target (reactively-sputtered AlN). Fig.3 shows cross sectional SEM images of two different types of the AlN film.

The TE property of the μTEGs is measured by approaching a micro thermostat to the AlN TC film. The thermostat is heated at 45 °C. The TE current was measured by applying loading voltage V_{load}. Upon the TE measurements, temperature difference across the SiNWs is monitored by an IR camera with a 8.4 μm spatial resolution.

3. Results and Discussions

Fig. 4 shows the relationship between the TE current I_{TE} and V_{load} and between TE power density P_{TE} and V_{load}. The short-circuit current (I_{SC}) and the maximum thermoelectric power (P_{max}) of the μTEGs with reactively-sputtered AlN are 4.13 μA cm^{-1} and 27.9 nW cm^{-2}, respectively. I_{SC} and P_{max} of μTEGs with nonreactively-sputtered AlN are 1.19 μA cm^{-1} and 2.78 nW cm^{-2}, respectively. The μTEG with reactively-sputtered AlN has higher I_{SC} and P_{max} than that of the μTEGs with nonreactively-sputtered AlN.

Fig. 5(a) shows a temperature distribution of the μTEG including a micro thermography image. Fig. 5(b) shows the temperature difference between both ends of the SiNWs of the μTEGs with two different AlN films. As shown in Fig. 5(b), the temperature difference occurs in the SiNWs of the μTEG with nonreactively-sputtered AlN and reactively-sputtered AlN are 50 mK and 240 mK, respectively. This implies that the parasitic thermal resistance is dramatically reduced by using the reactively-sputtered AlN.

Fig. 6 shows the X-ray diffraction (XRD) spectra of nonreactively-sputtered AlN and reactively-sputtered AlN. A very small full-width-half-maximam (FWHM) can be confirmed in reactively-sputtered AlN. This suggests that reactive-sputtered AlN film has a high c-axis orientation. Thus, the higher crystallinity of the AlN film is a possible origin of the reduction of parasitic thermal resistance.

4. Conclusions

We fabricated SiNW-based µTEGs with AlN TC film deposited by two different sputtering processes. The TE power of the µTEGs is improved by using an AlN film which is reactively sputtered in Ar/N_2 mixture gas using Al target. The temperature difference across the SiNWs becomes larger in the µTEGs with reactively-sputtered AlN TC film than in that with nonreactively-sputtered AlN TC film. XRD measurements show that reactively-sputtered AlN has a high crystallinity. This is considered to be the origin of the reduction of parasitic thermal resistance of the µTEGs. Our findings indicated that the crystallinity of TC film is important for achieving a high TE power generation density.

Acknowledgements

This work was supported by CREST, JST (JPMJCR15Q7). A part of this study was supported by NIMS Nanofabrication Platform in Nanotechnology Platform Project sponsored by the Ministry of Education, Culture, Sports, Science and Technology (MEXT), Japan.

References

[1] A. I. Hochbaum, et al., Nature, **451** (2008) 163.
[2] M. Totaro et al., Microelec. Eng., **97** (2012) 157.
[3] G. Pennelli, et al., Nanotechnol. **5**. (2014) 1268.
[4] S. Xie, et al., Polym. Test., **23** (2004) 794.
[5] H. Watanabe, et al., Int. J. Thermophys., **25** (2004) 221.

.

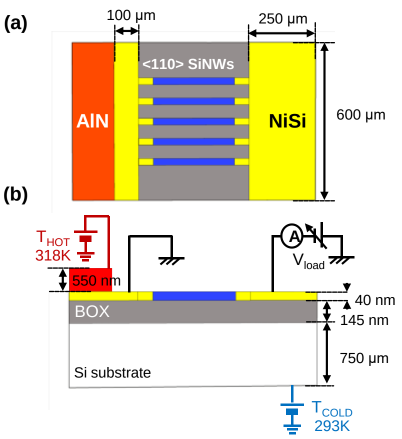

Fig.1 Schematic diagrams of our fabricated Si nanowire-based µTEG. (a) Top-view. (b) Side-view.

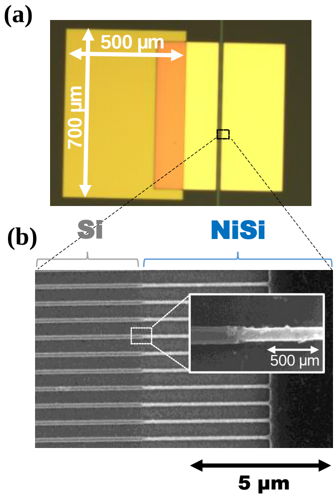

Fig.2 (a) Optical microscopy image of the µTEG, (b) SEM image of the Si nanowire (SiNW) and NiSi pad of the µTEG .

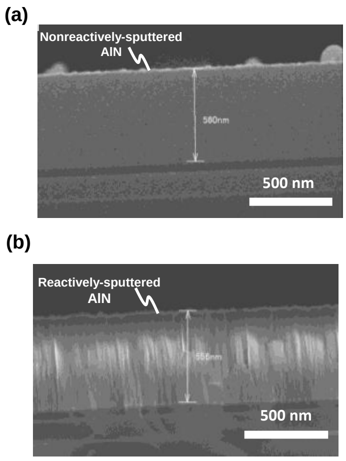

Fig.3 Cross-sectional images of two different types of AlN film. (a) Nonreactively-sputtered AlN (b) Reactively-sputtered AlN

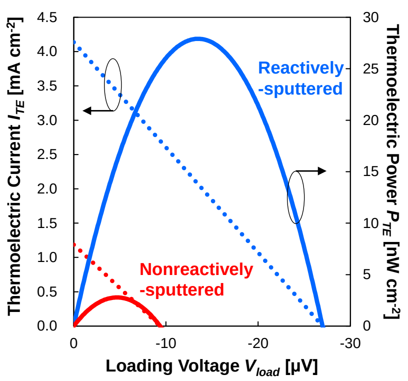

Fig.4 I_{TE}-V_{load} and P_{TE}-V_{load} characteristic of the µTEG with nonreactively-sputtered AlN TC film (red line) and reactively-sputtered AlN TC film (blue line).

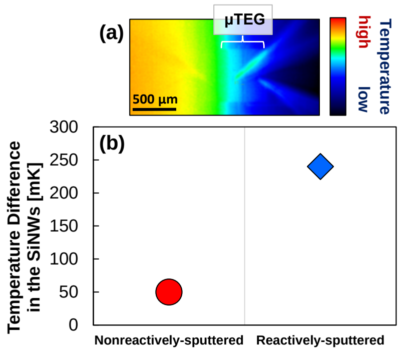

Fig.5 (a) Thermography image of the µTEG. (b) Temperature difference between both ends of the SiNWs of the µTEGs with two different types of AlN TC films.

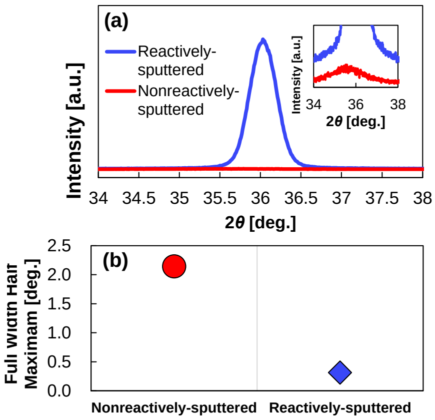

Fig.6 X-ray diffraction (XRD) measurement results. (a) XRD spectra of nonreactively-sputtered AlN film and reactively-sputtered AlN film. (b) Full width half maximam of the AlN (0002)